1994023384 N94-27887

Martian Atmospheric Radiation Budget

442632

Bernhard Lee Lindner

AER, Inc.

840 Memorial Drive

Cambridge, MA 02139

USA

Telephone:(617)349-2280

Fax:(617)661-6479

Submitted to Publications of the Astronomical Society of Japan

April 1993

Revised manuscript submitted October 1993

Second revision submitted January 1994

No. of Pages: 24

No. of Figures: 6

No. of Tables: 0

ABSTRACT

A computer model is used to study the radiative transfer of the martian winter-polar atmosphere. Solar heating at winter-polar latitudes is provided predominately by dust. For normal, low-dust conditions, CO_2 provides almost as much heating as dust. Most heating by CO_2 in the winter polar atmosphere is provided by the 2.7 μm band between 10 km and 30 km altitude, and by the 2.0 μm band below 10 km. The weak 1.3 μm band provides some significant heating near the surface. The minor CO_2 bands at 1.4, 1.6, 4.8 and 5.2 μm are all optically thin, and produce negligible heating. O_3 provides less than 10% of the total heating. Atmospheric cooling is predominantly thermal emission by dust, although CO_2 15 μm band emission is important above 20 km altitude.

Key Words: Mars, Radiative Transfer, Atmosphere, Planets

INTRODUCTION

While the past 20 years of spacecraft exploration have expanded our knowledge of the planet Mars, it seems more interesting problems exist today than ever before. At the heart of most of these mysteries is the winter polar atmosphere. Observations of the winter polar atmosphere have been limited by orbital constraints and darkness, and few models have been constructed to date. CO_2 and H_2O condensation commonly occur in the winter polar atmosphere of Mars, resulting in extensive cloudiness and a massive ice sheet. The structure and composition of the polar clouds as functions of latitude, altitude and season are poorly understood. Although observations of the southern polar hood are limited, it appears strikingly different from its northern counterpart, with much less coverage and different altitude structure (James, 1983; Christensen and Zurek, 1983; Martin and James, 1984; Akabane et al., 1990). The seasonal recession of the south polar cap (e.g., Iwasaki et al., 1990) cannot be accurately reproduced with energy balance models without consideration of atmospheric radiative effects (Narumi, 1980; James and North, 1982; Lindner, 1990; 1991a; 1992a; 1992b; 1993a), and the relative fraction of snow and frost in the cap is unknown (Pollack et al., 1990). Atmospheric dynamics at winter polar latitudes is also dependent on atmospheric heating and cooling (Haberle et al., 1979; 1982). Ozone abundances on Mars are also dependent on the radiative effects of dust (Lindner, 1988), and the observance of ozone on Mars is impaired by the radiative effects of dust (Lindner, 1992c).

Understanding the dominant radiative heating and cooling mechanisms in the winter polar atmosphere is crucial to solving many of these mysteries. While dynamical and latent heat mechanisms do provide as much as half of the atmospheric energy budget (Pollack et al., 1990), it is the radiative transfer mechanisms which drive the dynamical and latent heat mechanisms. In fact, due to the strong CO_2 heating and cooling, radiative processes are relatively more important in determining the temperature structure of the martian atmosphere than of the terrestrial atmosphere (e.g., Pollack et al., 1990). This work intends to establish the relative importance of O_3, CO_2 and dust in the radiative heating and cooling of the winter polar atmosphere of Mars, studying the importance of all wavelength bands. CO_2 was shown to be the only gas which produced appreciable infrared cooling at winter polar latitudes by Goody and Belton (1967), Crisp (1990), and Savijarvi(1991). Also, significant solar heating occurs in all the near-infrared (NIR) bands of CO_2 (Pollack et al., 1981; Lindner, 1985; Savijarvi,1991). Ozone was suggested to be an important contributor to the atmospheric temperature in the polar regions by Kuhn et al. (1979). However, the contribution of ozone to the atmospheric heat budget was later shown to be minor when compared to the contribution of dust (Lindner, 1991b). However, atmospheric heating due to dust absorption of solar radiation was shown to be important during dust storms by Gierasch and Goody (1972), Moriyama (1975), Zurek (1978), and Davies (1979). The importance of both CO_2 and dust in infrared radiative transfer, as well as the interaction between gas and dust, was demonstrated for certain cases by Kondrat'ev and Moscalenko (1975). The importance of both gas and dust in martian radiative transfer requires an advanced model capable of accurately handling the scattering by dust and the complex wavelength structure of carbon dioxide. To simplify the problem, most prior work has studied gas and dust radiative transfer separately and avoided their overlapping opacities, a technique which is inaccurate (Lindner, 1993b). To more properly assess the relative importance of dust and CO_2 in the thermal budget, this study treats them simultaneously.

MODEL

The discrete ordinate method of Stamnes et al. (1988) is used to treat the scattering, absorption and emission of monochromatic radiation through the martian atmosphere. The exponential sum program of Wiscombe and Evans (1977) and Evans et al. (1980) converts the banded wavelength structure of CO_2 to allow for monochromatic treatment (Lindner, 1985; 1993b; Lindner et al., 1990a,b). Lindner (1993b) clearly shows that errors as large as 50% occur when dust and CO_2 cooling and heating rates are computed separately and then summed. Hence, an approach such as the exponential sum technique which allows for simultaneous treatment of CO_2 and dust in the solution of the radiative transfer equation is necessary in order to properly assess their relative importance (Lindner, 1993b). Transmission functions for the 2.759, 4.301

and 14.93 μm bands of CO_2 (hereafter abbreviated as 2.7, 4.3, and 15.0, respectively) are taken from the line-by-line model results of Gal'tsev and Osipov (1979). The transmission function, Tr, as a function of temperature T, pressure P, and CO_2 column abundance U is extrapolated from the Gal'tsev and Osipov results (subscript G) to temperatures below 200 K by

$$Tr(T,P,U) = 1 - [(1 - Tr_G(200\ K, P, U))\ (T/200\ K)^Q] \qquad (1)$$

The exponential Q is found to be 0.45, 0.3, and 0.8 for the 2.7, 4.3, and 15 μm bands, respectively, when the temperature dependencies for the Pollack et al. (1981) transmission functions are recast in this form. Using a modified version of the FASCOD transmission model (Clough et al., 1986), the accuracy of these transmission functions is confirmed, and transmission functions are obtained for the 1.316, 1.455, 1.600, 2.020, 4.840 and 5.200 μm bands of CO_2 (hereafter abbreviated as 1.3, 1.4, 1.6, 2.0, 4.8, and 5.2, respectively) covering the range in temperature and pressure present in the atmosphere to 40 km altitude (Lindner et al., 1990a,b). Additionally, ozone absorption cross-sections from 1500 Å to 3200 Å (Daumont et al., 1983; Freeman et al., 1984) and from 4000 Å to 8000 Å (Griggs, 1968) and ultraviolet (UV) cross-sections for CO_2 (Shemansky, 1972; Lewis and Carver, 1983), O_2 (Demore et al., 1988), H_2O (Thompson et al., 1963; Hudson, 1971), HO_2 (Demore et al., 1988) and H_2O_2 (Demore et al., 1988) are included [e.g., Lindner, 1988; 1991b].

Dust opacities vary from 0.2 to 1.0 for conditions other than global dust storms (Pollack et al., 1979; Lumme and James, 1984). However, dust opacities over winter polar latitudes may be slightly less [e.g., Lindner, 1990]. A gaussian profile describes the vertical distribution of dust, being well-mixed to 20 km altitude for conditions other than global dust storms (Anderson and Leovy, 1978; Zurek, 1982; Korablev et al., 1993). Dust storm conditions are not considered here because of the dramatic increase in dynamical processes during dust storms. The wavelength dependence of the dust opacity is given by Toon et al. (1977). The single scattering albedo of airborne dust as a function of wavelength is given by Zurek (1978; 1982) and Toon et al. (1977) for solar and infrared wavelengths, respectively, using a solar average of 0.9 (Clancy and Lee, 1991). Scattering of radiation by dust is represented by the Henyey-Greenstein phase function (Toon et al., 1977; Clancy and Lee, 1991). Computational difficulties which accompany highly asymmetric phase functions are removed with the Delta-M method (Wiscombe, 1977). The emissivity of airborne dust is high and has been calculated as a function of wavelength from theory and observations (Toon et al., 1977; Simpson et al., 1981). Dust optical properties in the near-IR (1-5 μm) are highly uncertain, hence making the calculated heating and cooling rates uncertain. However, as will be shown later, dust heating and cooling rates in the near-IR are minor, making the uncertainty in dust optical properties in the near-IR unimportant. Dust optical properties in the 15 μm region are also highly uncertain, and factor of 2 uncertainty in the computed cooling rates is quite possible. Clouds will also affect atmospheric radiative transfer. However, since the cloud opacity is highly variable (i.e. Briggs and Leovy, 1974), the cloud particle scattering properties are very uncertain, and even the composition of the clouds is unclear, the effect of clouds is highly speculative and variable. But clouds should affect atmospheric radiative transfer similarly to how dust does, since dust single scattering albedos are very high (Lindner, 1990; 1993a).

The Rayleigh scattering optical depth is computed as in Hansen and Travis (1974), using parameters appropriate for Mars. Solar fluxes are taken from Smith and Gottlieb (1974) and Rottman (1981), after adjusting for the eccentricity and orbital radius of Mars. Solar heating rates are diurnally averaged (e.g., Cogley and Borucki, 1976). Atmospheric properties are zonally averaged and assumed azimuthally-independent. The region from the surface to 40 km altitude is broken into 20 2-km-thick layers to account for vertical inhomogeneity. The improved Curtis-Godson approximation (Yamamoto et al., 1972; Ramanathan and Coakley, 1978) is used to treat vertical inhomogeneity at thermal wavelengths. The Chapman function is used to approximate the slant path in place of the secant function [e.g., Smith and Smith, 1972], because the winter polar atmosphere always has large solar zenith angles, and the secant function is in error for large angles.

Atmospheric composition is taken as 95% CO_2 (Owen et al., 1977; see also Kondrat'ev et al., 1973). Atmospheric composition may have been quite different in past epochs, with CO_2

being perhaps a minor constituent (e.g., Lindner and Jakosky, 1985; Lindner, 1993c), but this study focuses on the present epoch. Season-dependent CO_2 abundances (Hess et al., 1980) are corrected for circulation-induced pressure gradients (Haberle et al., 1979) and elevation (Jakosky and Farmer, 1982; Lindal et al., 1979). The surface pressure is 8 mbar at 57°N latitude in late winter, which is when the maximum O_3 column abundance of 57 μm-atm was observed (Barth et al., 1973). The altitude dependence of O_3 is based on model results (Lindner, 1988).

As this study uses late northern winter conditions (L_s = 343°), the surface is covered by somewhat dirty ice with an albedo of 0.5 (Kieffer, 1979; James and Lumme, 1982). [Ls, the solar longitude, is a seasonal index; Ls of 0°, 90°, 180°, 270°, correspond to northern spring equinox, summer solstice, autumnal equinox, and winter solstice, respectively]. The wavelength dependence of the ice albedo is taken from Hapke et al. (1981) and Warren and Wiscombe (1980). The infrared (5.4 - 100 μm) albedo of the polar cap is assumed to be zero (Kieffer, 1970; Smythe, 1975; Wiscombe and Warren, 1980). An average ice emissivity of 0.9 is adopted, with the wavelength dependence given in Ditteon and Kieffer (1979) and Hunt et al. (1980). The temperature profile rises linearly with altitude from 150K at the surface to 160K at 10 km, and then falls linearly with altitude to 130 K and 40 km, typical for winter polar conditions (Lindal et al., 1979; Kieffer, 1979; Martin, 1984). Atmospheric temperatures are poorly known above 30 km altitude, and therefore results above that altitude are speculative and are not presented here. Local thermodynamic equilibrium is assumed (Gierasch and Goody, 1967; Uplinger et al., 1984; Hourdin, 1992).

RESULTS AND DISCUSSION

Figure 1 presents the ozone, carbon dioxide, and dust heating rates, and the carbon dioxide and dust cooling rates, for late winter (L_s = 343°) conditions at 57°N latitude with 0.2 vertical optical depths, τ_v, of dust (averaged over the solar spectrum). The net heating and net cooling are virtually identical at all altitudes. Because thermal emission is a strong function of the temperature and heating is virtually independent of temperature, less than a 10K adjustment in the assumed temperature profile will yield a perfect balance of heating and cooling. These modifications would still be consistent with observations of temperature (Lindal et al., 1979). Because the variation in dust with altitude is not well understood, the discrepancy could also be due to the assumed altitude profile of dust. Indeed, the assumed temperature profile could be correct, and the dust profile could be extracted by obtaining a balance between heating and cooling. Note that in addition to radiative cooling, energy could also go into condensation. In fact, clouds are often observed at these latitudes and seasons. Clouds would also change heating and cooling rates by increasing the flux (and heating) up high, and decreasing flux (and heating) in the lower 10 km.

While the near equality of heating and cooling rates means that meridional and vertical heat transport may not be required to explain the observed winter polar temperatures, it certainly does not rule out any meridional or vertical heat transport. Indeed, vertical heat transport could also be responsible for the low cooling rates at 20-30 km altitude. Observations do show some day to day variability, which could be due to changes in dynamical heat transport, or to pockets of high ozone or dust concentrations which would change radiative heating and cooling. However, maximum dynamical heating rates are of the order lK/day, with typical winter polar heating rates much smaller (Gadian, 1978; Pollack et al., 1981). While this could be significant near the surface, it becomes less so at higher altitudes.

The relative importance of gas and dust is clearly seen in Figure 1. Dust heating is the major source of heating at all altitudes, particularly above 20 km. Ozone provides approximately 10% of the total heating at all altitudes. 57 μm atmospheres of ozone are used, the maximum observed by Mariner 9 (Barth et al., 1973). [1 μm atmosphere = 2.69×10^{15} cm^{-2}]. Smaller ozone abundances will reduce the importance, but not dramatically. This contradicts earlier work by Kuhn et al. (1979) which showed ozone to be a more significant source of heating. However, Kuhn et al. (1979) ignored the heating by dust, which is clearly incorrect (Lindner, 1991b). Indeed, 0.2 vertical optical depths of dust represent the minimum amount of dust observed (Leovy et al., 1972; Pollack et al., 1979; Thorpe, 1981; Zurek, 1981). Larger dust loading will provide greater heating. Ozone heating is almost the same as that of the NIR bands of CO_2, at all altitudes. This occurs because the major CO_2 bands are saturated at the large solar zenith angles in the winter polar atmosphere.

Figure 1 can also be used to show what would happen to the thermal structure for the case of no dust. CO_2 and O_3 heating is triple CO_2 cooling near the surface, while CO_2 cooling is triple CO_2 and O_3 heating at 30 km altitude. This means that a dust-free atmosphere would be warmer near the surface and cooler at 30 km to allow for a balance between heating and cooling. Higher lapse rates were found in other dust-free studies as well (e.g., Gierasch and Goody, 1968).

Cooling rates are also dominated by dust. Dust cooling is greater than CO_2 15 μm band cooling from the surface to 25 km altitude, with CO_2 cooling dominant above this altitude. Note that cooling is not dependent on latitude, but on temperature. Hence the relative importance of dust cooling to CO_2 cooling is approximately the same at all winter polar latitudes.

The dominant ozone heating occurs at 2700 Å, with appreciable contributions from 2200 Å to 3100 Å (Lindner, 1991b). The Chappuis bands (4000 - 7000 Å) provide over 10% of the total ozone heating near the surface. CO_2, O_2, H_2O, HO_2, and H_2O_2 produce minor heating of the winter polar atmosphere at UV wavelengths, although CO_2 and O_2 UV heating is appreciable above 30 km altitude (Lindner, 1991b). H_2O, HO_2, and H_2O_2 number densities are too low for any appreciable UV heating.

CO_2 solar heating rates at near-infrared (NIR) wavelengths at 57°N latitude are computed for each CO_2 band, as shown in Figure 2. Most heating by CO_2 in the winter polar atmosphere is provided by the 2.7 μm band between 10 km and 30 km altitude, and by the 2.0 μm band below 10 km. The weak 1.3 μm band provides some significant heating near the surface. The minor CO_2 bands at 1.3, 1.4, 1.6, 4.8 and 5.2 μm are all optically thin, and produce negligible heating. The 2.0 μm band is more strongly absorbing than these minor bands and becomes optically thick at 10 km altitude, which results in a decreasing heating rate with a decrease in altitude below 10 km. The 2.7 μm band is stronger yet, and becomes optically thick at 20 km altitude. The 4.3 μm and 15 μm bands are very efficient, and are optically thick even at 30 km altitude. 15 μm band heating is surprisingly strong, despite the low solar flux at infrared wavelengths. The explanation lies in the large bandwidth (from 12 to 19 μm) and the efficient absorption over the band width.

In addition to being heated from absorption of solar radiation by O_3 and CO_2, the martian atmosphere is also heated by absorption of solar radiation by dust. As dust optical depths are not as strongly wavelength dependent as CO_2 and O_3 optical depths, the altitude dependence of dust heating is virtually the same for all wavelengths (Fig. 3). The strongest heating occurs in the visible where the maximum in solar flux occurs.

Atmospheric cooling rates due to thermal emission by 0.2 vertical optical depths of dust are presented in Figure 4. The maximum cooling occurs at 10 km altitude. Cooling is not as efficient in the lowest 5 km for two reasons. The temperature profile is inverted, with a maximum near 5-10 km altitude. Thus the near-surface atmosphere absorbs more radiation relative to its emission than does the atmosphere at 10 km altitude. Furthermore, the larger optical depths near the surface do not allow the emitted thermal radiation to escape the layer as easily as at higher altitudes.

The maximum cooling due to dust below 30 km altitude occurs in the 12-18 μm wavelength interval. This is due to the cold temperatures at winter polar latitudes. The overlap of strong dust cooling in the 12-18 μm interval with the strong cooling by CO_2 in the 15 μm band (12-19 μm) is particularly important, as discussed by Lindner (1993b). Hence, to properly account for both dust and CO_2 cooling, they must be treated simultaneously (Lindner, 1993b), unlike what is usually done. Significant cooling due to dust also occurs at wavelengths longer than 18 μm. Cooling by dust at wavelengths shorter than 12 μm is inefficient due to the cold winter polar temperatures. (Recall that the peak Planck emission occurs at longer wavelengths for colder temperatures.)

Cooling due to CO_2 near the surface occurs mostly in the wings of the 15 μm band, those parts of the 15 μm band where neither absorption nor emission is efficient. Photons emitted near the surface in the center of the 15 μm band (the strongly absorbing parts of the band) are rapidly re-absorbed. Hence, the cooling is smaller at lower altitudes (see Fig. 1) due to the inability of photons to escape and cool the atmosphere. Photons in the line center can escape to space more easily at higher altitudes, explaining the higher cooling rates there. Cooling to the surface also occurs, and is included in all calculations. However, in order to cool to the surface, photons must pass through large optical depths. Cooling to the surface is only important right near the surface.

Cooling rates in the 4.3 μm band of CO_2 increase from 10^{-6} K/Mars day at the surface to 3×10^{-4} K/Mars day at 30 km. Hence, cooling in the 4.3 μm band of CO_2 is about 10^{-3}% of the total cooling via CO_2. Clearly, 4.3 μm band cooling is not an important process in the winter polar atmosphere of Mars. The 4.3 μm cooling rate has the same altitude behavior as the 15 μm cooling rate. As with the 15 μm band, the line center is optically thick near the surface and all emitted photons are quickly reabsorbed, preventing effective line-center cooling in the 4.3 μm band. 4.3 μm cooling would be larger at warmer latitudes, as thermal emission would shift to shorter wavelengths. However, 4.3 μm band cooling will never be an important cooling source in the martian atmosphere. The 4.3 μm band and other NIR bands are important cooling processes in the Earth's atmosphere.

The heating and cooling rates for a late winter ($L_s = 343°$) atmosphere at 57° N latitude with more dust ($\tau_v = 0.5$) are shown in Fig. 5. Comparing Fig. 1 and Fig. 5, we see that dust heating and cooling rates increase at higher dust opacities, at all altitudes. Clearly, dust heating and cooling dominates over that of gas, except possibly for CO_2 cooling above 30 km altitude. As $\tau_v = 0.5$ was not unusual during the Viking mission, dust heating and cooling would dominate for most winter polar latitudes and seasons. Dust heating and cooling at larger dust loadings is even more dominant. During global dust storms (τ_v~3), heating and cooling by O_3 and CO_2 will be negligible compared to that of dust. However, dynamical transport of heat increases during dust storms.

For τ_v (dust) = 0.5, meridional and vertical heat transport may be even less important than for the $\tau_v = 0.2$ case. Based on observational and modeling evidence, meridional and vertical winds do not change much between the 0.2 and 0.5 cases (Haberle et al., 1982). Therefore, radiative equilibrium may be a more valid assumption at $\tau_v = 0.5$ because total radiative heating and cooling rates are twice as large for τ_v (dust) = 0.5, and are greater than 3 K/Mars day at almost all altitudes.

Heating and cooling rates are well balanced in the lower 20 km of the atmosphere in Fig. 5. Above 20 km the assumed temperatures are incorrect. Temperatures closer to 140 K at 30 km altitude would give a better balance between the heating and cooling rates above 20 km. Indeed, the inability of dust cooling to keep up with dust heating at higher dust loadings in addition to heat transport is the explanation for the higher atmospheric temperatures observed during global dust storms. The explanation lies in the negative feedback of larger dust loadings, in that larger opacities decrease the ability of photons to escape. CO_2 cooling also becomes less effective at higher dust loadings due to dust-gas interaction (Lindner, 1993b).

Obviously, higher dust loading results in increased dust heating rates. The higher optical depth chokes off some light from reaching lower altitudes, which explains why the increases in the heating rate for higher dust optical depths are not as large at the surface as at higher altitudes. Cooling rates for 0.5 vertical optical depths of dust are twice the cooling rates for $\tau_v = 0.2$. While the optical depth is 2.5 times as large, cooling rates are only 2.2 times larger. This is because two negative feedbacks exist in that larger optical depths also hinder the ease of escape for emitted photons, and in that larger optical depths increase the thermal flux which increases absorption and heating. The thermal heating at altitudes above 25 km also increases. The heating above 25 km increases because the upward thermal flux is larger for $\tau_v = 0.5$, which results in larger absorption in the upper atmosphere, while the thermal emission above 25 km remains the same.

The phenomenon of thermal heating is also partly responsible for the low lapse rates in the martian atmosphere. Because dust and CO_2 are both radiatively active in the infrared, the atmosphere near the surface is able to cool very effectively, and keep near-surface temperatures low. But the high thermal fluxes are also causing a heating as they are absorbed by the other regions of the atmosphere. Any part of the atmosphere that is too cold will be heated by both solar and thermal flux. Higher dust loading increases both solar and thermal heating more effectively than thermal cooling. This results in more isothermal conditions as the dust loading increases, as is observed.

Figure 6 shows the heating and cooling rates deeper in the winter polar region at 70°N latitude for the same season for normal, low-dust conditions. The cooling rates are the same as at 57°N latitude (Figure 1), because the same temperature profile is used. The same temperatures are used at both latitudes to illustrate latitude-dependent changes in the heating rates. The lower solar fluxes at 70°N latitude (due to the larger solar zenith angle) result in lower heating rates. The atmospheric heating and cooling is approximately equal near the surface and above 20 km. However, the assumed temperature inversion is too strong for radiative equilibrium for 70°N latitude conditions, as the cooling at 10 km is twice the heating. Slightly lower temperatures in the 5-10 km range would provide a better balance between heating and cooling, and would agree with observational evidence (Lindal et al., 1979). Dynamics could be relatively more important at transporting heat at 70°N latitude because the heating rates are lower. However, observations and dynamical modeling indicate that the atmosphere is even more stable against motion at these latitudes which would lower heat transport (Haberle et al., 1979).

The excess cooling could also go into condensation, rather than in changing the temperature (Pollack et al., 1990). Indeed, optically thick clouds are frequently observed in the 5-10 km altitude range. As the atmospheric temperature near the surface is already at the CO_2 condensation temperature, the clouds at this latitude will be at least partly composed of CO_2 ice. Clouds would also alter the heating rate profile by shifting the location of solar flux through scattering.

Comparing Fig. 1 and Fig. 6 shows that the relative importance of O_3 to CO_2 heating is virtually the same at 70°N latitude as it is at 57°N latitude. However, both O_3 and CO_2 heating are less important relative to dust. CO_2 heating occurs mostly in bands which are optically thick. At higher latitudes, the larger solar zenith angles only serve to decrease the transmission in these already optically-thick bands and hence decrease their relative importance. O_3 is less important to the heat budget at 70°N latitude due to the lower O_3 abundances there (Barth et al., 1973; Lane et al., 1973; Lindner, 1991b). The same general altitude and wavelength behavior in heating and cooling is seen at 70°N latitude as at 57°N latitude. Therefore, while dust heating is less at higher latitudes due to the decreased solar flux, the importance of dust heating relative to gas heating has increased.

The large solar zenith angle Θ at 70°N latitude increases the effective optical depth ($\tau = \tau_v/\cos\Theta$) of dust, which increases the absorption of solar flux, and hence increases the heating. The larger solar zenith angle also decreases the solar flux, and hence decreases the heating. In an optically-thin medium, these effects would cancel and the heating would be the same at 70°N latitude as at 57°N latitude. However, the 0.2 vertical optical depths of dust yield an effective optical depth of 1.7 at 70°N latitude. Thus, the dust is actually choking off the solar-flux, which decreases the heating rate relative to 57°N latitude. The lower heating at the surface is due to the large optical-depth of dust.

CO_2 NIR heating at 70°N latitude is half that at 57°N latitude. The general behavior of each band at 70°N latitude is similar to that at 57°N latitude, although the bands saturate at higher altitudes. Consequently, the 4.3 and 15 µm bands are less important at 70°N latitude, and the 2.0 and 2.7 µm bands are less important near the surface. The minor bands (1.3, 1.4, 1.6, 4.8 and 5.2 µm) are optically thin at 70°N latitude, as at 57°N latitude. The heating in all bands is reduced at 70°N latitude, due to the lower solar flux (via the larger solar zenith angle). Comparing the results of 57°N latitude and 70°N latitude, it is apparent that CO_2 NIR heating would be markedly higher at equatorial latitudes, due to the increased solar flux, and the larger contributions by the saturated 2.0, 2.7, 4.3 and 15 µm bands. Hence, the relative importance of dust and CO_2 will shift in the favor of CO_2 at more equatorward latitudes. O_3 heating will not be important at equatorial and mid-latitudes because negligible ozone abundances exist there (Barth et al., 1973). Total heating rates will increase with decreasing latitude due to the decrease in the solar zenith angle. The net result is higher atmospheric temperatures with decreasing latitude, which is in fact observed.

SUMMARY AND CONCLUSIONS

Heating in the winter polar atmosphere of Mars is provided mostly by dust at visible wavelengths, especially for high dust loading, or at high latitudes. CO_2 NIR heating is always less than dust heating at 57°N latitude during late winter, but is comparable to dust heating at low altitudes for minimal dust loading. CO_2 NIR heating is more important at equatorial latitudes, and less important at high latitudes. Most CO_2 heating comes from the 2.7 μm band above 10-20 km altitude, with most heating by the 2.0 μm band below. 1.3 μm band heating is appreciable near the surface. The importance of minor CO_2 bands requires their inclusion in models of polar winter winds and surface energy balance. Ozone heating is only 10% of the total heating at 57°N latitude, and is even less at other latitudes due to lower ozone abundances. Ozone heating was suggested to be important to the polar heat budget by Kuhn et al. (1979), but the importance of dust heating was ignored by Kuhn et al. Heating by CO_2, O_2, H_2O, HO_2 and H_2O_2 is negligible at ultraviolet wavelengths below 30 km altitude.

CO_2 15 μm band cooling is the dominant source of cooling at high altitudes for low dust abundances, but is ineffective near the surface. CO_2 4.3 μm band cooling is negligible. Dust cooling is the dominant source of cooling at winter polar latitudes under most conditions, with the largest dust cooling in the 12-18 μm wavelength range. Dust cooling increases at higher dust loadings; however dust cooling does not increase as fast as dust heating, due to several negative feedbacks. As a result, atmospheric temperatures rise with increasing dust opacity, in agreement with observations. The warmest winter polar temperatures occur during global dust storms, when the largest dust opacity exists. However, whether the high temperatures at polar latitudes during global dust storms are due primarily to radiative processes or dynamical heat transport is uncertain. Radiative effects of dust have little effect on the overall recession of the polar cap (Lindner, 1990).

Radiative processes are responsible for the low lapse rates in the martian atmosphere. Significant dust and gas heating occurs at all altitudes, damping out inhomogeneities in temperature. Any region of the atmosphere which is significantly colder than the rest of the atmosphere is warmed not only by solar flux but also by the absorption of the large thermal flux. Large lapse rates are quickly eliminated by solar and infrared heating. As atmospheric dust loading increases, the atmosphere becomes more isothermal due to the increased solar and thermal heating, particularly at higher altitudes. Ignoring dust altogether leads to the opposite situation. CO_2 cools ineffectively near the surface, but cools readily at high altitudes, which leads to stronger lapse rates in the dust-free atmosphere.

Acknowledgments

My thesis advisor, Gary Thomas, was invaluable in pointing out errors and improvements in the radiative transfer. Knut Stamnes and Warren Wiscombe are thanked for providing their computer codes. The reviewers are thanked for insightful comments on this manuscript. This work was funded by NSF grant ATM 8305841 and NASA grants NASW-4614, NAGW-389 and NAGW-552.

REFERENCES

Akabane, T., K. Iwasaki, Y. Saito, and Y. Narumi, Blue clearing of Syrtis Major at the 1982 Opposition, J. Geophys. Res., 95, 14649-14655, 1990.

Anderson, E. and C. Leovy, Mariner 9 television limb observations of dust and ice hazes on Mars, J. Atmos. Sci., 35, 723734, 1978.

Barth, C.A., C.W. Hord, A.I. Stewart, A.L. Lane, M.L. Dick and G.P. Anderson, Mariner 9 Ultraviolet experiment: Seasonal variation of ozone on Mars, Science, 179, 795-796, 1973.

Briggs, G.A. and Leovy, C.B., Mariner 9 observations of the Mars north polar hood, Bull. Amer. Met. Soc., 55, 278-296, 1974.

Christensen, P.R. and R.W. Zurek, Martian water-ice clouds: Location and seasonal variation, Bull. Amer. Astron. Soc., 15, 847, 1983.

Clancy, R.T., and S.W. Lee, A new look at dust and clouds in the Mars atmosphere: Analysis of emission-phase-function sequences from global Viking IRTM observations, Icarus, 93, 135-158, 1991.

Clough, S.A., F.X. Kneizys, E.P. Shettle, and G. P. Anderson, Atmospheric Radiation and Transmission, FASCOD2, Proceedings of the Sixth Conference on Atmospheric Radiation, Williamsburg, Virginia, 1986

Cogley, A.C. and W.J. Borucki, Exponential approximations for daily average solar heating or photolysis, J. Atmos. Sci., 33, 1347-1356, 1976.

Crisp, D., Infrared radiative transfer in the dust-free martian atmosphere, J. Geophys. Res., 95, 14577-14588, 1990.

Daumont, D., J. Brion and J. Malicet, Measurement of total atmospheric ozone: Consequences entailed by new values of ozone absorption cross-sections at 223 K in the 310-350 nm spectral range, Planet. Space Sci., 31, 1229-1234, 1983.

Davies, D.W., Effects of dust on the heating of Mars surface and atmosphere, J. Geophys. Res., 84, 8289-8293, 1979.

DeMore, W.B., J.J. Margitan, M.J. Molina, R.T. Watson, D.M. Golden, R.F. Hampson, M.J. Kurylo, C.J. Howard, and A.R. Ravishankara, Chemical kinetics and photochemical data for use in stratospheric modeling, evaluation no. 7, JPL Publication 85-67, Jet Propulsion Laboratory, Pasadena, California, 1985.

Ditteon, R. and H.H. Kieffer, Optical properties of solid carbon dioxide: Application to Mars, J. Geophys. Res., 84, 8294-8300, 1979.

Evans, J.W., W.B. Gragg and R.J. LeVeque, On the least squares exponential sum approximation with positive coefficients, Math. of Computat., 34, 203-211, 1980.

Freeman, D.E., K. Yoshino, J.R. Esmond and W.H. Parkinson, High resolution absorption cross-section measurements of ozone at 195 K in the wavelength region 240-350 nm, Planet. Space Sci., 32, 239-248, 1984.

Gadian, A.M., The dynamics of and the heat transfer by baroclinic eddies and large-scale stationary topographically forced long waves in the martian atmosphere, Icarus, 33, 454-465, 1978.

Gal'tsev, A.P. and V.M. Osipov, Spectral transmission functions of CO2 for the conditions of the martian atmosphere, Bull. (Izv.), Acad. Sci. USSR, Atmos. Ocean. Phys., 15, 767-769, 1979.

Gierasch, P.J. and R.M. Goody, An approximate calculation of radiative heating and radiative equilibrium in the martian atmosphere, Planet. Space Sci., 15, 1465-1477, 1967.

Gierasch, P.J. and R.M. Goody, A study of the thermal and dynamical structure of the martian lower atmosphere, Planet. Space Sci., 16, 615-646, 1968.

Gierasch, P.J. and R.M. Goody, The effect of dust on the temperature of the martian atmosphere, J. Atmos. Sci., 29, 400 - 402, 1972.

Goody, R. and M.J.S. Belton, Radiative relaxation times for Mars. A discussion of martian atmospheric dynamics, Planet. Space Sci., 15, 247-256, 1967.

Griggs, M., Absorption coefficients of ozone in the ultraviolet and visible regions, J. Chem. Phys., 49, 857-859, 1968.

Haberle, R.M., C.B. Leovy and J.B. Pollack, A numerical model of the martian polar cap winds, Icarus, 39, 151-183, 1979.

Haberle, R.M., C.B. Leovy and J.B. Pollack, Some effects of global dust storms on the atmospheric circulation of Mars, Icarus, 50, 322-367, 1982.

Hansen, J.E. and L.D. Travis, Light scattering in planetary atmospheres, Space Science Reviews, 16, 527-610, 1974.

Hapke, B., E. Wells, J. Wagner and W. Partlow, Far-UV, Visible, and Near-IR reflectance spectra of frosts of H_2O, CO_2, NH , and SO_2, Icarus, 47, 361-367, 1981.

Hess, S.L., J.A. Ryan, J.E. Tillman, R.M. Henry and C.B. Leovy, The annual cycle of pressure on Mars measured by Viking Landers 1 and 2, Geophys. Res. Lett., 7, 197-200, 1980.

Hourdin, F., A new representation of the absorption by the CO2 15 micron band for a martian general circulation model, J. Geophys. Res., 97, 18319-18335, 1992.

Hudson, R.D., Critical review of ultraviolet photoabsorption cross sections for molecules of astrophysical and aeronomic interest, Rev. Geophys. Space Phys., 9, 305-406, 1971.

Hunt, G.E., E.A. Mitchell, H.H. Kieffer and R. Ditteon, Scattering-and absorption properties of carbon dioxide ice spheres in the region 360-4000 cm^{-1}, J. Quant. Spectrosc. Radiat. Transfer, 24, 141-146, 1980.

Iwasaki, K., Y. Saito, Y. Nakai, and T. Akabane, Martian south polar cap 1988, J. Geophys. Res., 95, 14751-14754, 1990.

Jakosky, B.M. and C.B. Farmer, The seasonal and global behavior of water vapor in the Mars atmosphere: Complete global results of the Viking atmospheric water detector experiment, J. Geophys. Res., 87, 2999-3019, 1982.

James, P.B., Condensation phase of the martian south polar cap, Bull. Amer. Astron. Soc., 15, 846-847, 1983.

James, P.B. and K. Lumme, Martian south polar cap boundary: 1971 and 1973 data, Icarus, 50, 368-380, 1982.

James, P.B. and G.R. North, The seasonal CO_2 cycle on Mars: An application of an energy balance climate model, J. Geophys. Res., 87, 10271-10283, 1982.

Kieffer, H.H., Spectral reflectance of CO2-H2O frosts, J. Geophys. Res., 75, 501-509, 1970.

Kieffer, H.H., Mars south polar spring and summer temperatures: A residual CO_2 frost, J. Geophys. Res., 84, 8263-8288, 1979.

Kondrat'ev, K.Ya., and N.I. Moscalenko, The spectral and spatial structure of a thermal radiation field unde the conditions of Mars' turbid atmosphere, Dokl. Akad. Nauk SSSR, 224, 316-319, 1975. (English translation: Sov. Phys. Dokl., 20, 593-594, 1976).

Kondrat'ev, K.Ya., Yu.M.Timofeev, O.M. Pokrovskii and T.A. Dvorovik, Determination of vertical temperature profile in the atmosphere of Mars from Mariner 9 infrared thermal radiation measurements, Dokl. Akad. Nauk SSSR, 211, 801-803, 1973. (English translation: Sov. Phys. Dokl., 18, 509-510, 1974).

Korablev, O.I., V.A. Krasnopolsky, A.V. Rodin, and E. Chassefiere, Vertical structure of martian dust measured by solar infrared occulatations from the Phobos spacecraft, Icarus, 102, 76-87, 1993.

Kuhn, W.R., S.K. Atreya and S.E. Postawko, The influence of ozone on martian atmospheric temperature, J. Geophys. Res., 84, 8341-8342, 1979.

Lane, A.L., C.A. Barth, C.W. Hord and A.I. Stewart, Mariner 9 ultraviolet spectrometer experiment: Observations of ozone on Mars, Icarus, 18, 102-108, 1973.

Leovy, C.B., G.A. Briggs, A.T. Young, B.A. Smith, J.B. Pollack, E.N. Shipley and R.L. Wildey, The martian atmosphere: Mariner 9 television experiment progress report, Icarus, 17, 373-393, 1972.

Lewis, B.R. and J.H. Carver, Temperature dependence of the carbon dioxide photoabsorption cross section between 1200 and 1970 Angstroms, J. Quant. Spectrosc. Radiat. Transfer, 30, 297-309, 1983.

Lindal, G.F., H.B. Hotz, D.N. Sweetnam, Z. Shippony, J.P. Brenkle, G.V. Hartsell, R.T. Spear and W.H. Michael, Jr., Viking radio occultation measurements of the atmosphere and topography of Mars: Data acquired during 1 martian year of tracking, J. Geophys. Res., 84, 8443-8456, 1979.

Lindner, B. L., The aeronomy and radiative transfer of the martian atmosphere, Ph.D. Dissertation, 470 pp., University of Colorado, Boulder, 1985.

Lindner, B. L., Ozone on Mars: The effects of clouds and airborne dust, Planet. Space Sci., 36, 125-144, 1988.

Lindner, B. L., The martian polar cap: Radiative effects of ozone, clouds, and airborne dust, J. Geophys. Res., 95, 1367-1379, 1990.

Lindner, B. L., Why is the north polar cap on Mars different than the south polar cap?, Summaries, International Symposium on the Physics and Chemistry of Ice, p. 120-121, held in Sapporo Japan, Sept. 1-6, 1991a.

Lindner, B. L., Ozone heating in the martian atmosphere, Icarus, 93, 354-361, 1991b.

Lindner, B. L., Sunlight penetration through the martian polar caps: Effects on the thermal and frost budgets, Geophys. Res. Lett., 19, 1675-1678, 1992a.

Lindner, B. L., CO_2-ice on Mars: Theoretical simulations, in Physics and Chemistry of Ice, N. Maeno and T. Hondoh, ed.s, pp. 225-228, Hokkaido University Press, Sapporo, 1992b.

Lindner, B. L., Does UV instrumentation effectively measure ozone abundance?, in Workshop on innovative instrumentation for the in situ study of atmosphere-surface interactions on Mars, B. Fegley, Jr. and H. Waenke, ed.s, pp. 10-11, LPI Tech. Rep. #92-07, Part 1, Lunar and Planetary Institute, Houston, Texas, 1992c.

Lindner, B. L., The hemispherical asymmetry in the martian polar caps, J. Geophys. Res., 98, 3339-3344, 1993a.

Lindner, B. L., Cooling the martian atmosphere: The spectral overlap of the CO2 15 micron band and dust, accepted by Planet. Space Sci., 1993b.

Lindner, B. L., Comment on "Mars secular obliquity change due to the seasonal polar caps" by David Parry Rubincam, submitted to J. Geophys. Res., 1993c.

Lindner, B. L. and B. M. Jakosky, Martian atmospheric photochemistry and composition during periods of low obliquity, J. Geophys. Res., 90, 3435-3440, 1985.

Lindner, B. L., T. P. Ackerman, and J. B. Pollack, An efficient and accurate technique to compute the absorption, emission, and transmission of radiation by the martian atmosphere, in Scientific results of the NASA-sponsored study project on Mars: Evolution of volcanism, tectonics and volatiles, S.C. Solomon, V.L. Sharpton, and J.R. Zimbelman, ed.s, p. 198-200, LPI Tech. Rpt. 90-06, 322 pp., Lunar and Planetary Institute, Houston, Texas, 1990a.

Lindner, B. L., T. P. Ackerman, J. B. Pollack, O. B. Toon, and G. E. Thomas, Solar and IR radiation near the martian surface: A parameterization for CO_2 transmittance, In Lunar and Planetary Science XXI, pp. 696-697, Lunar and Planetary Institute, Houston, Texas, 1990b.

Lumme K. and P.B. James, Some photometric properties of the martian south polar cap region during the 1971 apparition, Icarus, 58, 363-376, 1984.

Martin, L.J., North polar hood observations during martian dust storms, Icarus, 26, 341-352, 1975.

Martin, L.J., Clearing the martian air: The troubled history of dust storms, Icarus, 57, 317-321, 1984.

Martin, L.J. and P.B. James, Mars 1984: The transition from polar hood to surface-cap (abstract), Bull. Amer. Astron. Soc., 16, 673, 1984.

Moriyama, S., Effects of dust on radiation transfer in the martian atmosphere. II. Heating due to absorption of the visible solar radiation and importance of radiative effects of dust on the Martian meteorological phenomena, J. Meteorl. Soc. Japan, 53, 214-221, 1975.

Narumi, Y., The seasonal variation of atmospheric pressure on Mars, in Proceedings of the 13th Lunar and Planetary Symposium, pp. 31-41, Institute of Space and Aeronautical Science, University of Tokyo, 1980.

Owen, T., K. Biemann, D.R. Rushneck, J.E. Biller, D.W. Howarth, and A.L. Lafleur, The composition of the atmosphere at the surface of Mars, J. Geophys. Res., 82, 4635-4639, 1977.

Pollack, J.B., D.S. Colburn, F.M. Flasar, R. Kahn, C.E. Carlston and D. Pidek, Properties and effects of dust particles suspended in the martian atmosphere, J. Geophys. Res., 84, 2929-2945, 1979.

Pollack, J.B., C.B. Leovy, P.W. Greiman and Y. Mintz, A martian general circulation experiment with large topography, J. Atmos. Sci., 38, 3-29, 1981.

Pollack, J.B., R.M. Haberle, J. Schaeffer, and H. Lee, Simulations of the general circulation of the martian atmosphere, 1, Polar processes, J. Geophys. Res., 95, 1447-1474, 1990.

Ramanathan, V. and J.A. Coakley, Jr., Climate modeling through radiative-convective models, Rev. Geophys. Space Phys., 16, 465-489, 1978.

Rottman, G.J., Rocket measurements of the solar spectral irradiance during solar minimum, 1972-1977, J. Geophys. Res., 86, 6697-6705, 1981.

Savijarvi, H., Radiative Fluxes on a dustfree Mars, Beitr. Phys. Atmosph., 64, 103-112, 1991.

Shemansky, D.E., Carbon dioxide extinction coefficient 1700-3000 Angstroms, J. Chem. Phys., 56, 1582-1587, 1972.

Simpson, J.P., J.N. Cuzzi, E.F. Erickson, D.W. Strecker, and A.T. Tokunaga, Mars: Far-infrared spectra and thermal-emission models, Icarus, 48, 230-245, 1981.

Smith, E.V.P. and D.M. Gottlieb, Solar flux and its variations, Space Sci. Rev., 16, 771-802, 1974.

Smith, F.L., III, and C. Smith, Numerical evaluation of Chapman's grazing incidence integral ch(X,X), J. Geophys. Res., 77, 3592-3597, 1972.

Smythe, W.D., Spectra of hydrate frosts: Their application to the outer solar system, Icarus, 24, 421-427, 1975.

Stamnes, K., S. Tsay, W. Wiscombe, and K. Jayaweera, Numerically stable algorithm for discrete-ordinate-method radiative transfer in multiple scattering and emitting media, App. Optics, 27, 2502-2509, 1988.

Thompson, B.A., P. Harteck and R.R. Reeves, Jr., Ultraviolet absorption coefficients of CO_2, CO, O_2, H_2O, N_2O, NH_3, NO, SO_2, and CH_4 between 1850 and 4000 Angstroms, J.

Geophys. Res., 68, 6431-6436, 1963.

Thorpe, T.E., Mars atmospheric opacity effects observed in the northern hemisphere by Viking orbiter imaging, J. Geophys. Res., 86, 11419-11429, 1981.

Toon, O.B., J.B. Pollack and C. Sagan, Physical properties of the particles composing the martian dust storm of 1971-1972, Icarus, 30, 663-696, 1977.

Uplinger, W.G., G.A. Ely, T.C. James and J.B. Kumer, Martian horizon radiance profiles (abstract), EOS, 65, 982, 1984.

Warren, S.G. and W.J. Wiscombe, A model for the spectral albedo of snow. II: Snow containing atmospheric aerosols, J. Atmos. Sci., 37, 2734-2745, 1980.

Wiscombe, W.J., The delta-m method: Rapid yet accurate radiative flux calculations for strongly asymmetric phase functions, J. Atmos. Sci., 34, 1408-1422, 1977.

Wiscombe, W.J. and J.W. Evans, Exponential-sum fitting of radiative transmission functions, J. Computational Phys., 24, 416-444, 1977.

Wiscombe, W.J. and S.G. Warren, A model for the spectral albedo of snow. I: Pure snow, J. Atmos. Sci., 37, 2712-2733, 1980.

Yamamoto, G., M. Aida and S. Yamamoto, Improved Curtis-Godson approximation in a non-homogeneous atmosphere, J. Atmos. Sci., 29, 1150-1155, 1972.

Zurek, R.W., Solar heating of the martian dusty atmosphere, Icarus, 35, 196-208, 1978.

Zurek, R.W., Inference of dust opacities for the 1977 martian great dust storms from Viking Lander 1 pressure data, Icarus, 45, 202-215, 1981.

Zurek, R.W., Martian great dust storms: An update, Icarus, 50, 288-310, 1982.

Figure Captions

Figure 1. Total atmospheric radiative heating and cooling as a function of altitude on Mars at 57°N latitude with τ_v (dust) = 0.2. Also shown is the contribution by CO_2, O_3 and dust.

Figure 2. Total solar heating rates for CO_2 as a function of altitude and the contribution by each CO_2 band (labeled by wavelength in μm) at 57°N latitude (a) and 70°N latitude (b).

Figure 3. Total radiative heating rate as a function of altitude due to absorption of solar radiation by dust (τ_v = 0.2) and the contribution from each wavelength bin from 0 to 5 microns (bins labeled on figure in μm).

Figure 4. Total infrared radiative cooling rate by dust as a function of altitude for τ_v = 0.2, and the contribution from each wavelength interval from 5 to 40 μm (wavelength range of each bin is labeled in μm).

Figure 5. As in Figure 1 except for τ_v (dust) = 0.5.

Figure 6. As in Figure 1 except at 70°N latitude for τ_v (dust) = 0.2

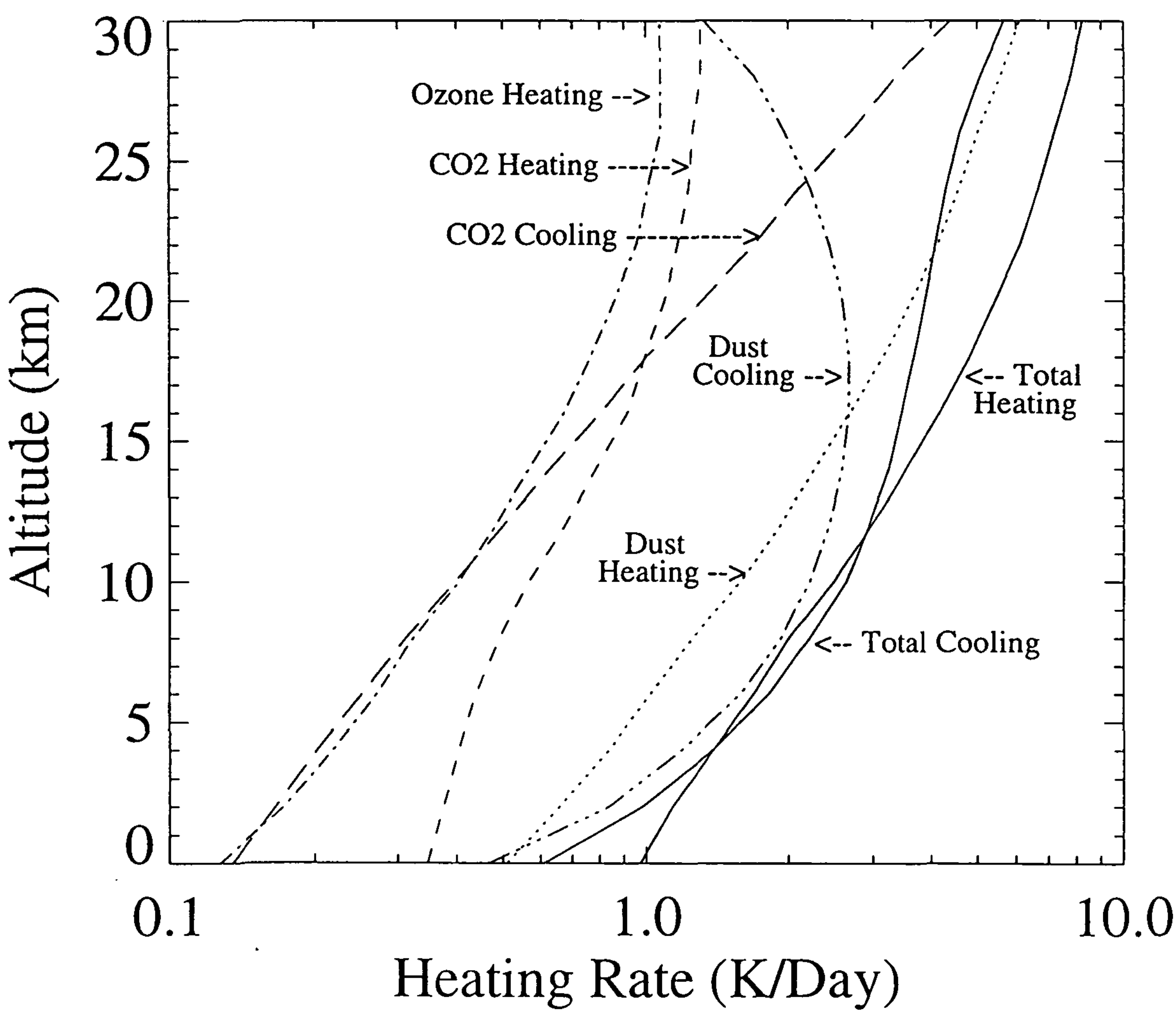

30
25
20
15
10
5
0
0.1
1.0
10.0
Altitude (km)
Heating Rate (K/Day)
Ozone Heating -->
CO2 Heating ------>
CO2 Cooling ------------>
Dust
Cooling -->
<-- Total
Heating
Dust
Heating -->
<-- Total Cooling

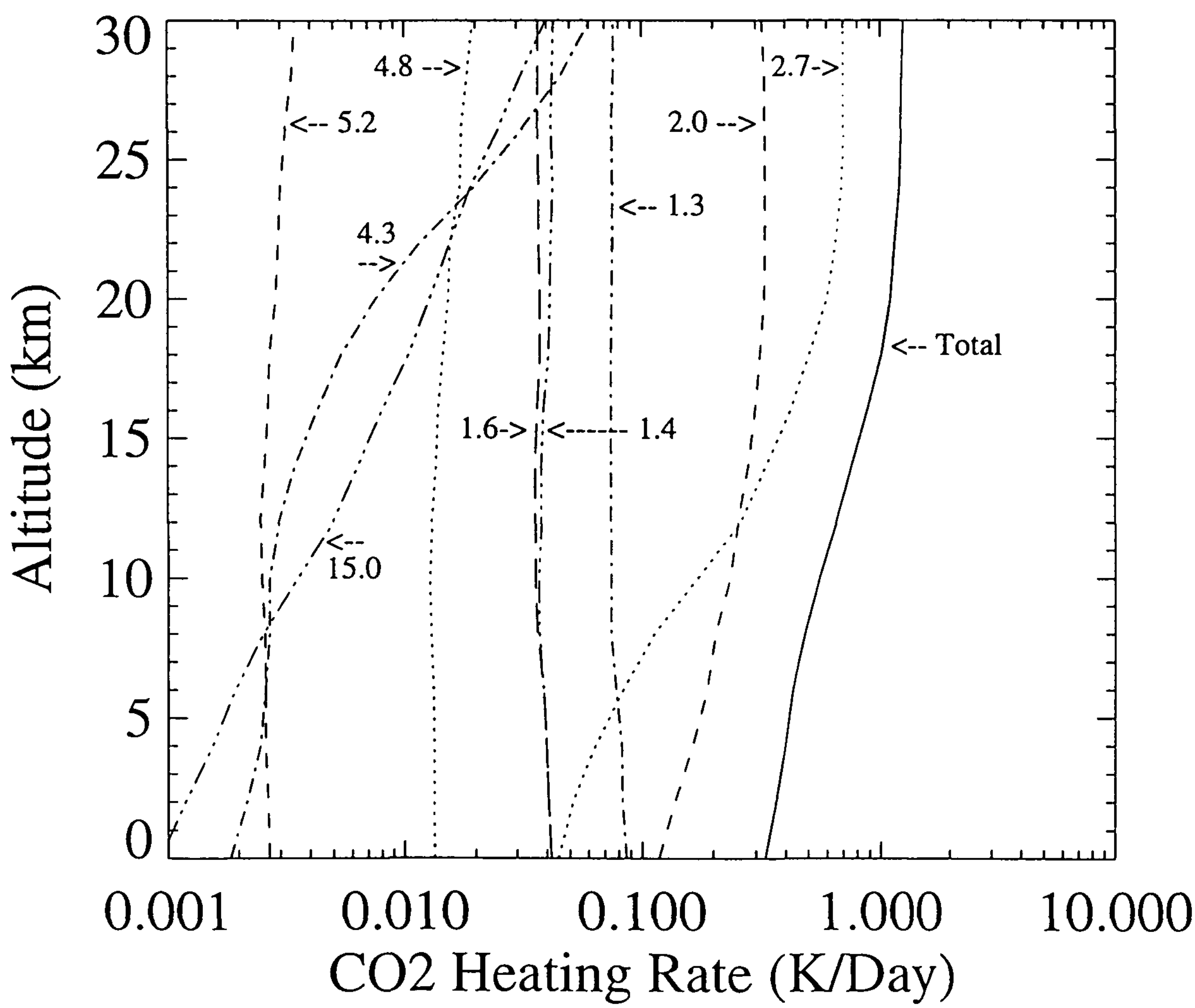

30
25
20
15
10
5
0
Altitude (km)
0.001
0.010
0.100
1.000
10.000
CO2 Heating Rate (K/Day)
4.8 -->
<-- 5.2
2.0 -->
2.7->
<-- 1.3
4.3
-->
<-- Total
1.6->
<------- 1.4
<--
15.0

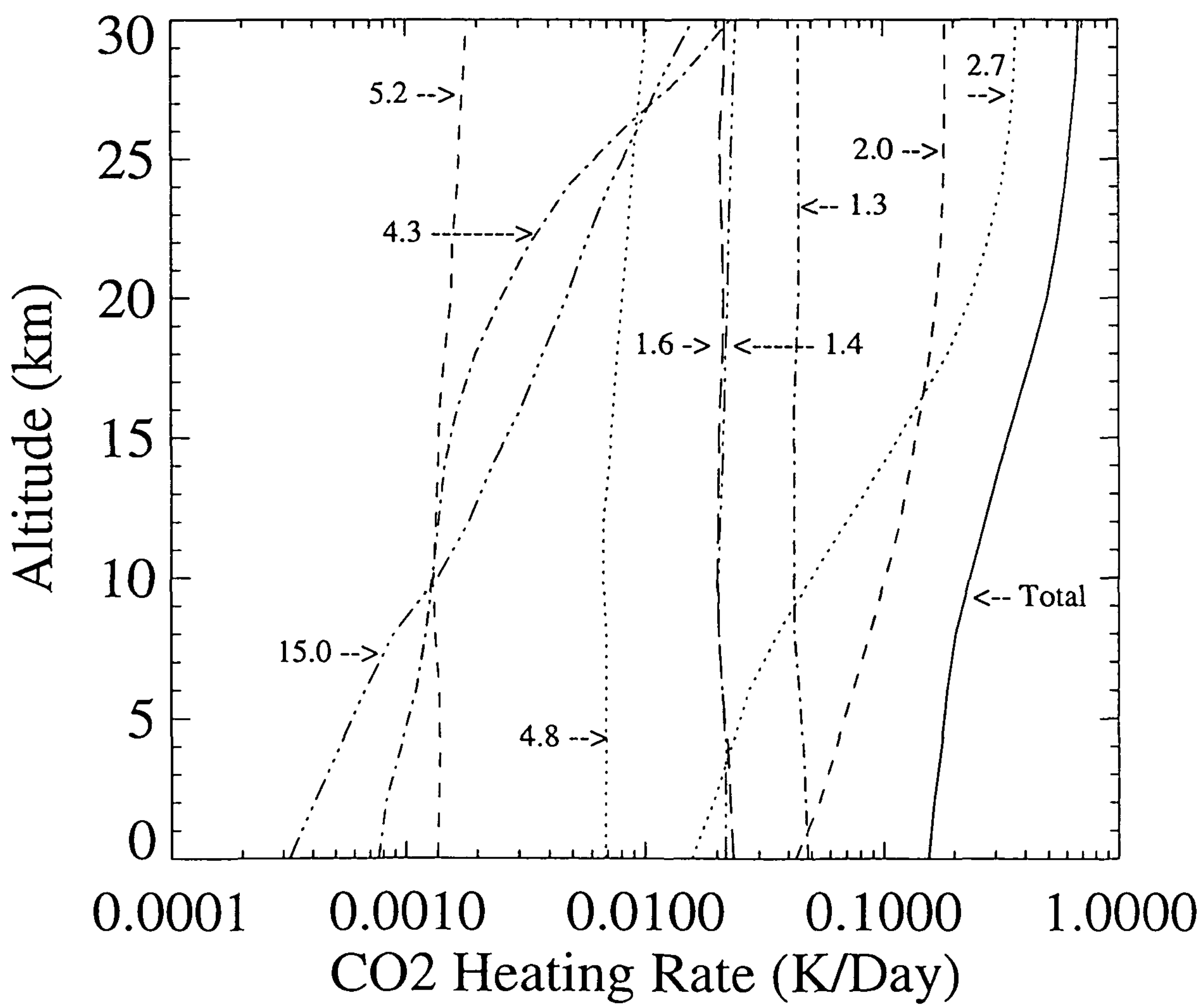

30
25
20
15
10
5
0
Altitude (km)
0.0001
0.0010
0.0100
0.1000
1.0000
CO2 Heating Rate (K/Day)
5.2 -->
4.3 ------->
15.0 -->
4.8 -->
1.6 ->
<------ 1.4
<-- 1.3
2.0 -->
2.7
-->
<-- Total

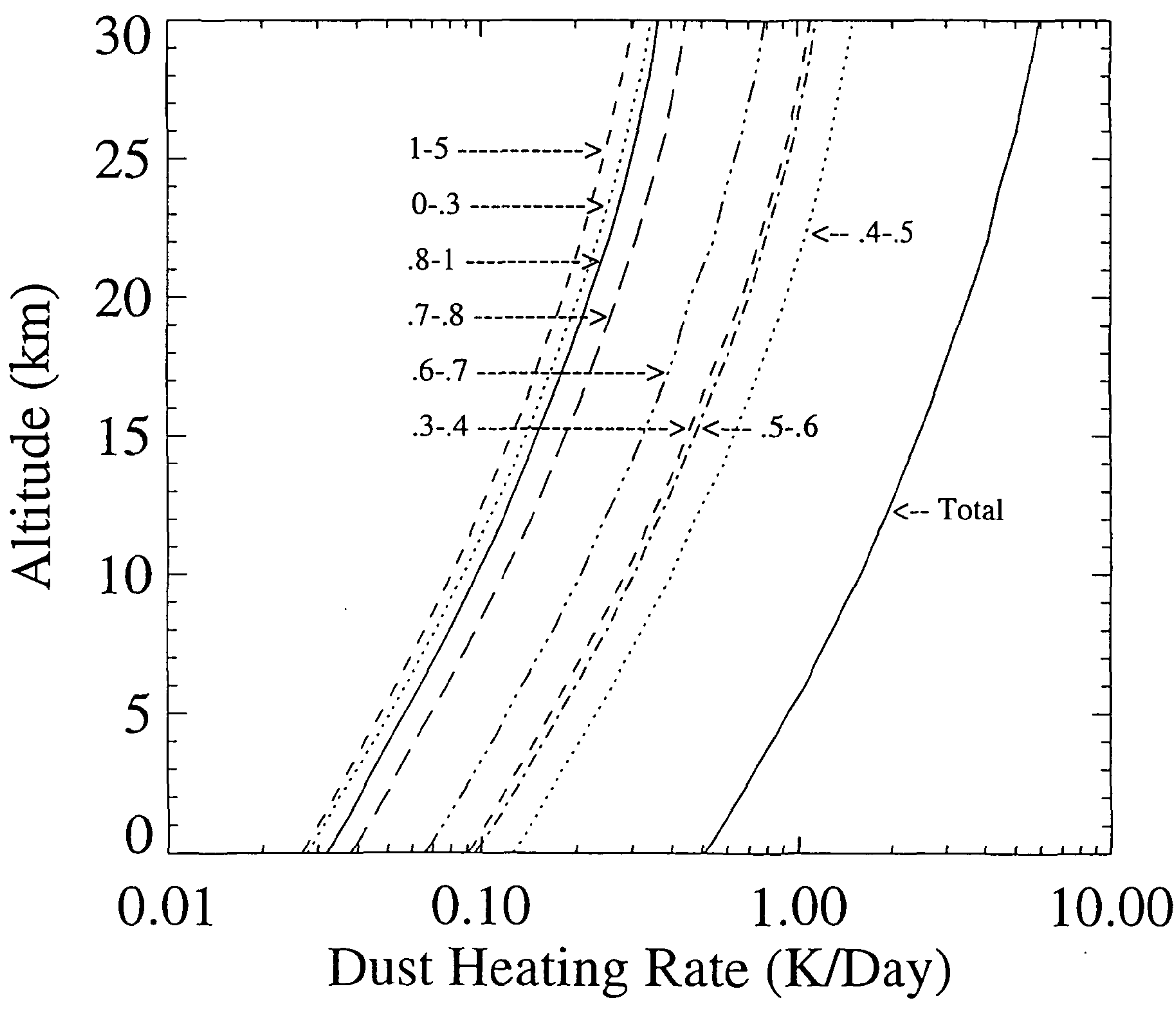

30
25
20
15
10
5
0
Altitude (km)
0.01
0.10
1.00
10.00
Dust Heating Rate (K/Day)
1-5
0-.3
.8-1
.7-.8
.6-.7
.3-.4
.5-.6
.4-.5
Total

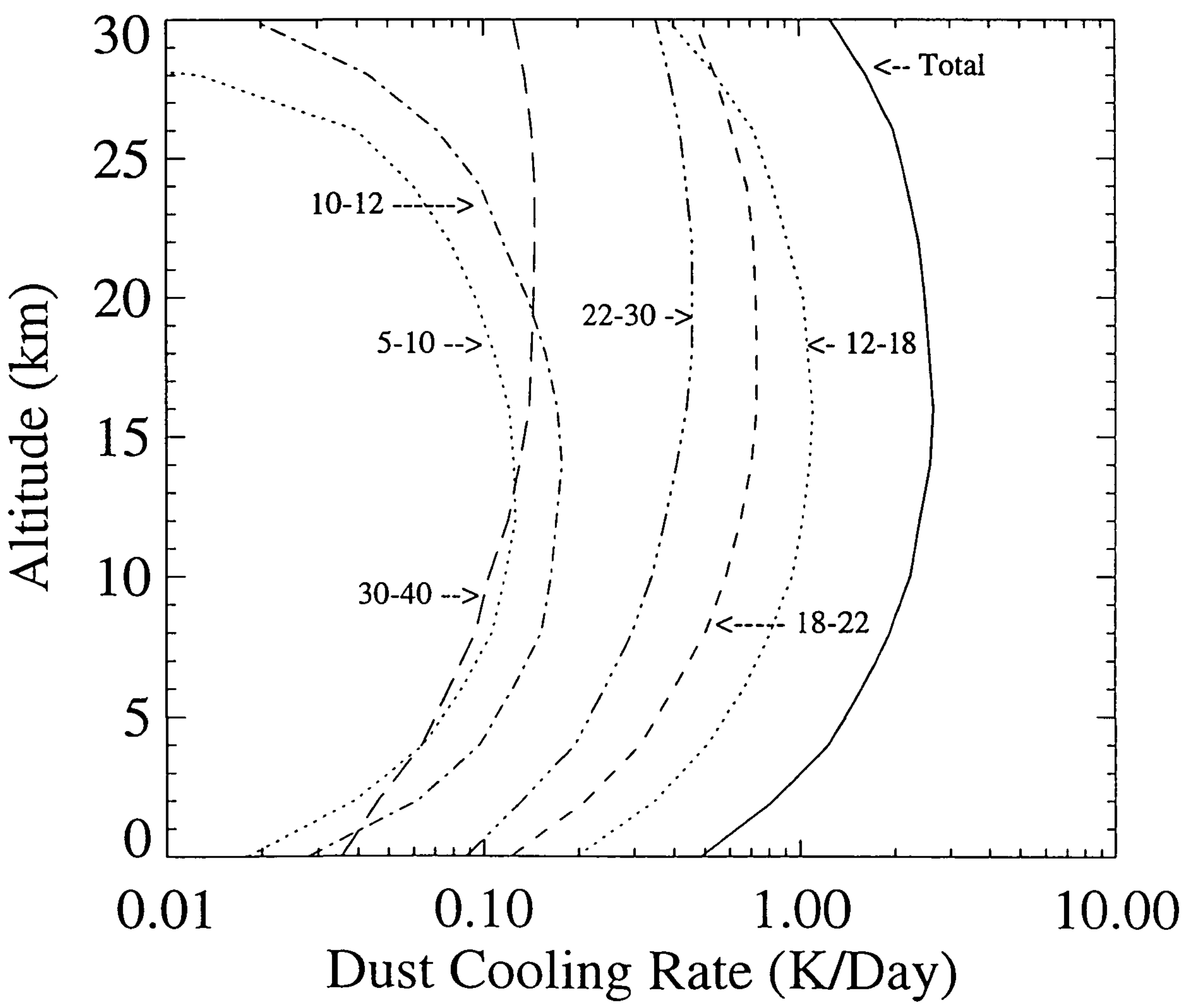

30
25
20
15
10
5
0
Altitude (km)
0.01
0.10
1.00
10.00
Dust Cooling Rate (K/Day)
<-- Total
10-12 ------->
5-10 -->
22-30 ->
<- 12-18
30-40 -->
<------ 18-22

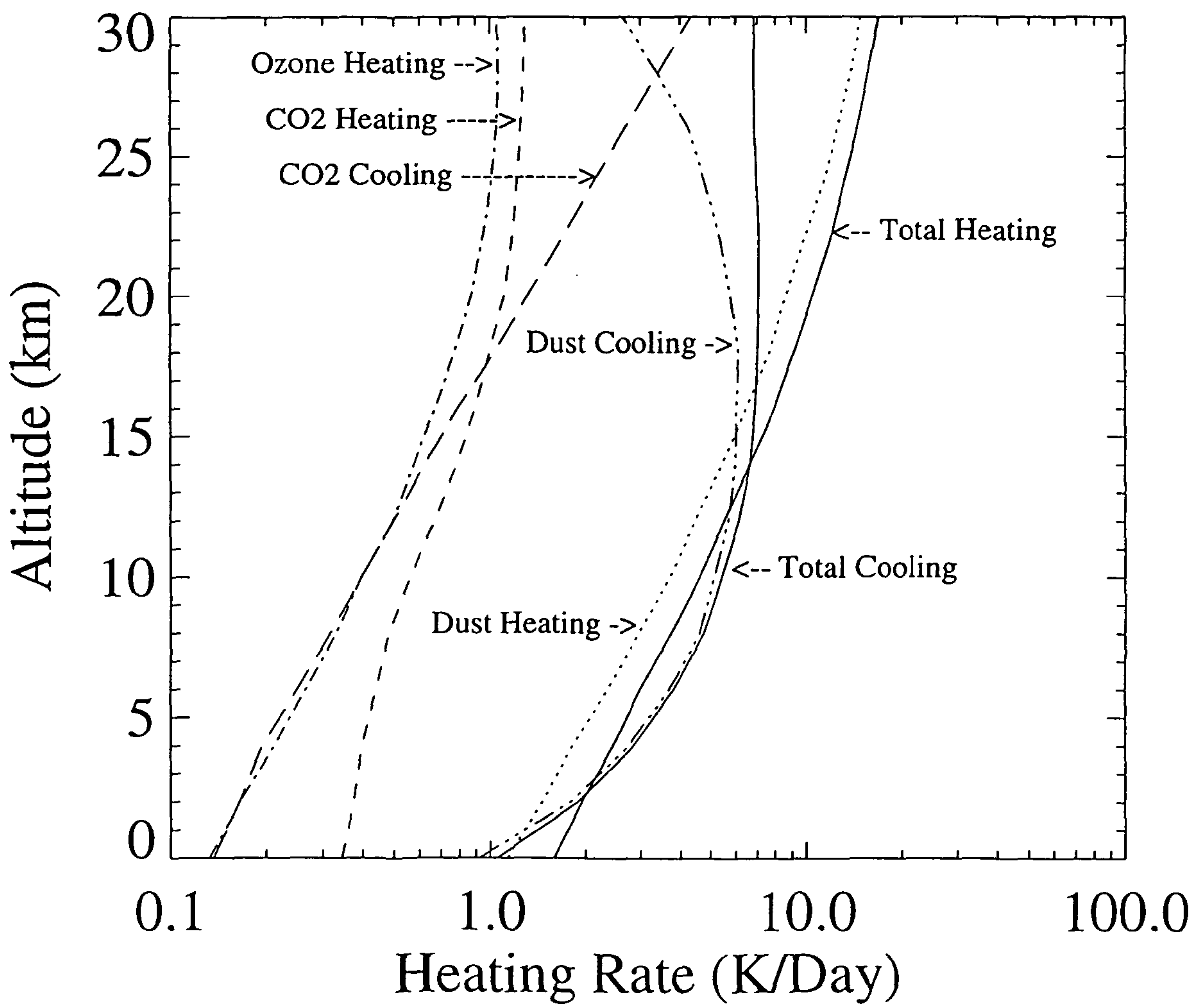

Ozone Heating -->
CO2 Heating ----->
CO2 Cooling ------------->
<-- Total Heating
Dust Cooling ->
<-- Total Cooling
Dust Heating ->
Altitude (km)
Heating Rate (K/Day)
0
5
10
15
20
25
30
0.1
1.0
10.0
100.0

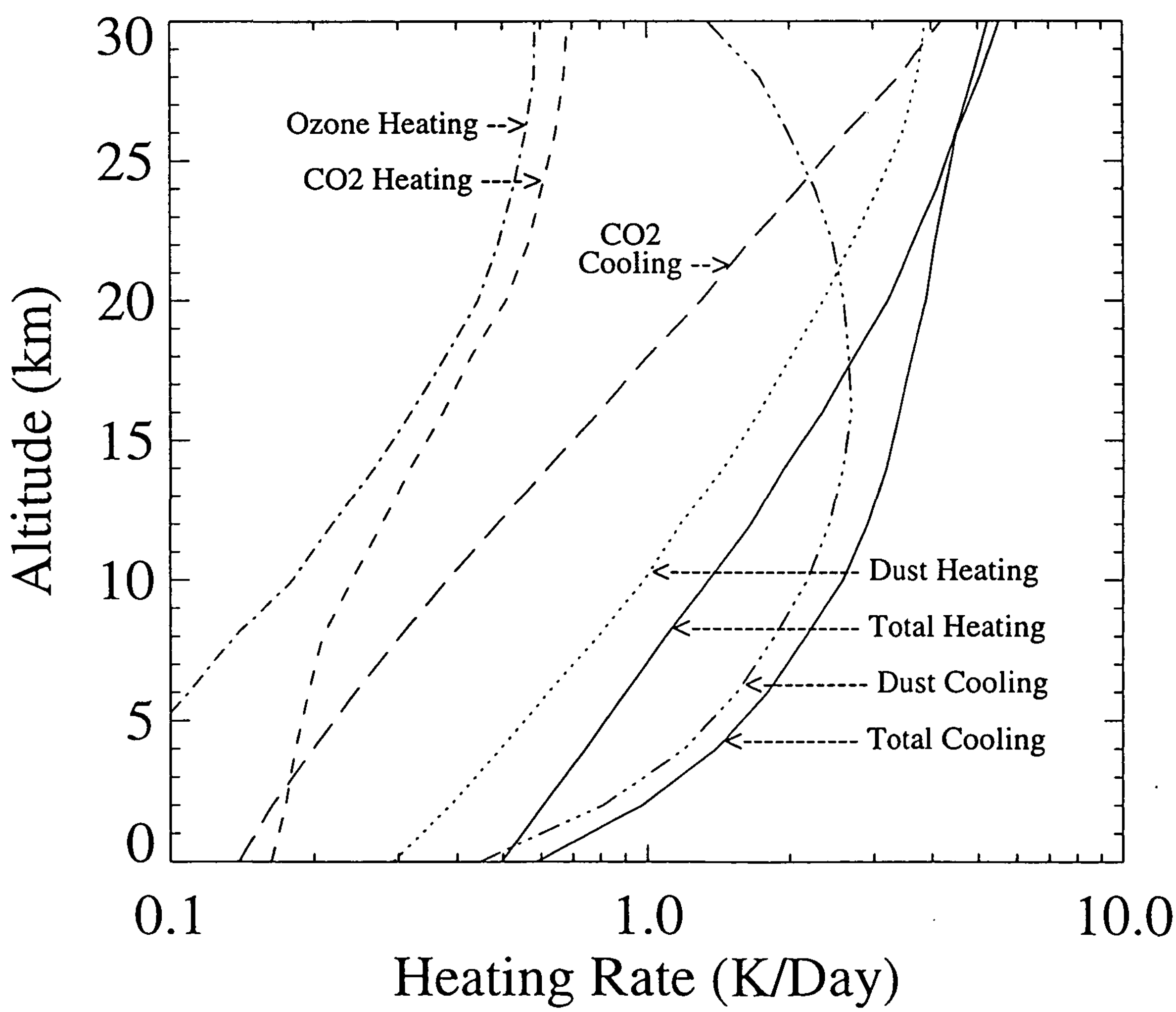

Ozone Heating -->
CO2 Heating --->
CO2
Cooling -->
Dust Heating
Total Heating
Dust Cooling
Total Cooling
30
25
20
15
10
5
0
Altitude (km)
0.1
1.0
10.0
Heating Rate (K/Day)